

Studies on Defluoridation of Water by Tea Ash: An Unconventional Biosorbent

NABA KUMAR MONDAL*, RIA BHAUMIK, TANMOY BAUR,
BISWAJIT DAS, PALAS ROY and JAYANTA KUMAR DATTA

Department of Environmental Science, The University of Burdwan, Burdwan-713104, India
Naba Kumar Mondal, Department of Environmental Science,
The University of Burdwan, 713104, India
nabakumar_mondal@indiatimes.com

Received 8 May 2012 / Accepted 28 May 2012

Abstract: Residual part of tea as a household waste was effectively used for removal of fluoride from aqueous medium. The variable operating parameters such as pH, initial fluoride concentration, sorbent particle size, agitation time and temperature. The defluoridation capacity increases with increasing adsorbent dose and contact time but decrease with initial concentration of fluoride solution. Moreover, acidic pH (6) showed the highest removal of fluoride. Further defluoridation follows second order kinetics and Langmuir and Freundlich adsorption isotherm. The surface and sorption characteristics were analyzed using FTIR and SEM techniques. For domestic and industrial applications, defluoridation with 100% achievement and subsequent regeneration of adsorbent was performed with a household water filter and fixed bed column respectively.

Keywords: Fluoride removal, Batch study, Tea residue, Isotherm study, Thermodynamic study

Introduction

Fluoride is one of the most potent groundwater pollutant¹. Excess intake (>1.5 mgL⁻¹) may cause fluorosis (dental, skeletal and non-skeletal) along with various neurological complication. Removal of fluoride from the ground water is challenging task among the scientists. Various technologies already developed to remove fluoride from drinking water by coagulation, membrane filtration, ion exchange, *etc.* But due to high cost for processing such technology is unfit for developing country. Therefore there is a great need for environmental friendly and low cost technology. One such low cost technology is adsorption and which is effective for removal of fluoride¹. Many low cost adsorbents such as Tamarind seed¹; Tamarind gel; Duck weed spirodela polyrrhiza were used for removal of fluoride.

Fluoride is known to be a natural contaminant for ground water resources globally¹. The removal of fluoride from water is one of the most important issues due to its ill-effects on human health and environment². According to World Health Organization³ the maximum permissible limit of fluoride concentration in drinking water is 1.5 mg L⁻¹. There are lot of methods developed for removal of excess fluoride from drinking water, such as the use of ion exchange columns, coagulation, use of membranes and electrochemical methods, the high cost of these technologies makes them unpractical for developing countries⁴. Among these techniques, adsorption seems to be an effective, environmentally friendly economical one⁵. Over the last few years numbers of investigations have been conducted to test the low cost adsorbent for fluoride removal such as activated alumina⁶, titanium-rich bauxite⁷, manganese oxide-coated alumina⁸ and carbon nanotubes⁹. Moreover, plant materials like serpentine and Tamarind gel¹⁰; Tamarind seed¹, Duck weed Spirodela Polyrhiza¹¹; *Hydrilla Verticillata*, Royale Plants¹² are also reported to accumulate fluoride and hence application as defluoridation agents has been suggested. The utilization of agricultural waste materias is increasingly becoming a vital concern because these wastes represent unused resources and in many cases present serious disposal problems.

Numerous waste biomass sources are available in different parts of the world, on which some experimental adsorption properties have been reported *e.g.* rice husk¹³, rice husk ash¹⁴, egg shell¹⁵, peanut shells¹⁶, corn cobs¹⁷, saw dust¹⁸, coir dust¹⁹, dry tree leaves and barks²⁰, tea and coffee waste²¹⁻²², rice and wheat bran²³⁻²⁴ and sea weeds²⁵. From the literature review it is learnt that the biosorptive defluoridation study is limited and hence in the present work is performed with the tea residue. This work investigates the potential of tea waste from nearest shop for removal of fluoride ions from aqueous solutions. The optimum operating conditions drawn equilibrium data and sorption kinetics for fluoride removal using water washed tea waste were obtained. Batch studies were conducted to ascertain practical applicability. Using both laboratory aqueous solution and groundwater field samples, the study aims to devise a simple, cheap and viable defluoridation method that could be adopted easily by village communities and urban dwellers.

Experimental

The tea residue collected from nearest teashop in local market of Burdwan Municipality, Burdwan Municipality, West Bengal, India was used for the experiments. Soluble and coloured components were removed from tea by washing with boiling water. This was repeated until the water was virtually colourless. After thoroughly washing, the adsorbent was sun dried and it is burned in muffle furnace (Paragon, Model no. PTC-1) at 500 °C for 30 minutes and dried tea ash was sieved and stored in sealed polythene bags. The activated tea ash powder (AcTAP) material was subjected to various physicochemical parameters and used for sorption. The fraction 50 µm was used for all the experiments except for the effect of particle size tests.

Instrument used for adsorbent characterization

The surface area of the adsorbent was measured by a surface area analyzer (Quantasorb Model, Qs. 7). The porosity and density of the adsorbent were determined by mercury proximate and specific gravity bottles, respectively elemental analysis was carried out with Perkin Elmer 2400 CHN Elemental Analyzer. Adsorbent surface characterized by FTIR analysis (PERKINELMER, FTIR, Model-RX1 Spectrometer). The pH of the solution was

measured by using digital pH meter (model no. Systronic-335). Fluoride was measured by ion selective electrode (Thermo Orion 370 PerpHecT Ion Selective Benchtop Meter), Scanning electron microscope was done by (HITACHI, S-530, Scanning Electron Microscope and ELKO Engineering, B.U., BURDWAN).

Determination of zero point charge

The zero surface charge characteristics of the tea ash were determined by using the solid addition method²⁶. 50 mL of 0.1 M KNO₃ solution was transferred to series of 100 mL conical flasks. The initial pH (pH₀) of the solutions was roughly adjusted from 1.0 to 10.0 by adding either fixed strength of HNO₃ (0.05) or 0.1N KOH. Then 1.5 g of AcTAP was added to each flask which was securely capped immediately. The flasks were then placed into a constant temperature water bath shaker and shaken for 24 h. The pH values of the supernatant liquid were noted after 24 h.

Synthetic contaminated water preparation

A synthetic solution of fluoride was prepared from analytical grade sodium fluoride (MERC, Bombay) and stored in polythene (TARSON made) bottle. The pH of the solution was adjusted to the required level, using HCl (0.1 N) and NaOH (0.1 N) solutions.

Batch adsorption studies

Adsorption experiments were carried out for the determination of pH, adsorbent dose variation, equilibrium time and kinetics, selection of an isotherm, effect of temperature and evaluation of thermodynamic parameters. The influence of pH (2.0-10.0), adsorbent concentration (0.2-2.4 g L⁻¹) and particle size (200-350 μm), contact time (40, 60, 120, 180, 240 and 300 min), initial fluoride concentration (1.5, 5.0, 7.0, 10.0, 15.0, 35.0 and 50.0 mg L⁻¹) and temperature (303, 313, 323 and 333 K) were evaluated during the present study in a 250 mL Erlenmeyer flasks and 100 mL of fluoride solution of known concentration was added for constant shaking (at 300 rpm) during 1hr in a temperature controlled magnetic stirrer at 303 ± 1K and then the solids were separated through filtration. The solutions were collected for analysis and fluoride concentration in the solution was determined by using ion selective meter. Each experiment was conducted three times and average values are reported. Control experiments, performed without addition of adsorbent, confirmed that the sorption of fluoride on the walls of Erlenmeyer flasks was negligible. The amount of fluoride adsorbed per unit adsorbent (q_e) (mg g⁻¹) was calculated according to a mass balance on the fluoride concentration using Eq. (1):

$$q_e = \frac{(C_i - C_e)V}{m} \quad (1)$$

Where, V = Volume (L) of the equilibrated solution, m = Mass of the adsorbent (g), C_i = Initial concentration of metal ion (mg L⁻¹), C_e = Equilibrium concentration of Fe⁺² (mg L⁻¹). The percent removal (%) of dyes was calculated using the following equation:

$$\text{Removal}(\%) = \frac{(C_i - C_e)}{C_i} \times 100 \quad (2)$$

Results and Discussion

Characterization of adsorbent

The physicochemical characteristics of tea ash are given in (Table 1). The surface characteristics make it suitable for sorptive defluoridation. The sorption is characterized under determination of zero point charge (pH_{ZPC}) of the adsorbent. Adsorption of cation is favored at pH > pH_{ZPC}, while the adsorption of anion is favored at pH < pH_{ZPC} (Figure 1)²⁶.

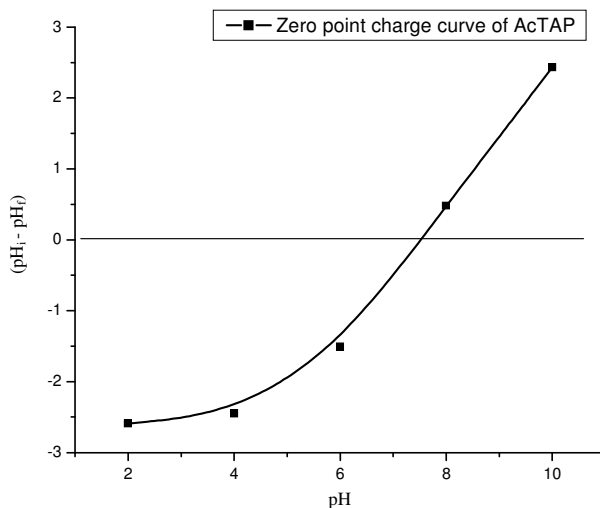


Figure 1. Zero Point charge of AcTAP

FTIR spectra of tea ash before and after F⁻ adsorption are shown in Figure 2a and b respectively. The band at 3427 cm⁻¹ is due to O-H vibration of aliphatic alcohol and the two peaks at 2853 cm⁻¹ and 2925 cm⁻¹ indicate the presence alkane C-H stretching. A significant shift of the peak from 796 cm⁻¹ to 875 cm⁻¹ occurs probably due to the aromatic C-H bond get disturbed by fluoride. The band at 1097 cm⁻¹ is due to stretching vibration of C-OH group of carboxylic acid. The band at 1097 cm⁻¹ is also shifted to 1094 cm⁻¹ after F⁻ adsorption. Scanning electron microscopy (SEM) observation (Figure 3a, 3b and 3c) shows rough surface of the adsorbent that provides large surface area for adsorption. Although adsorbent showed no change in its morphology after F⁻ adsorption. The micrograph (Figure 3c) very similar to Figure 3a indicated that the regeneration of fluoride from adsorbent surface has been occurred.

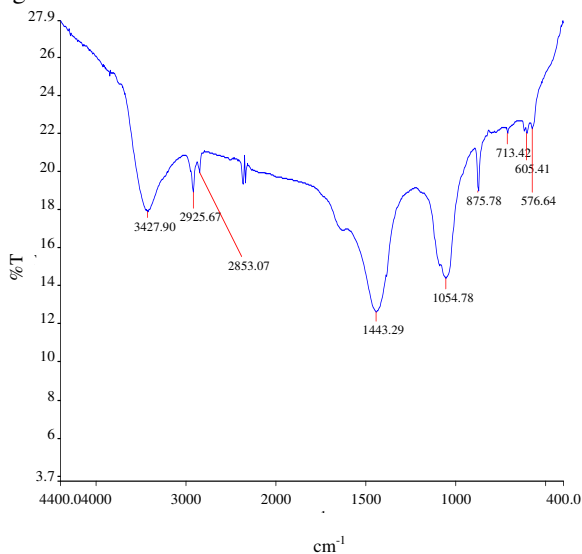


Figure 2a. IR Spectrum of AcTAP (before fluoride loaded)

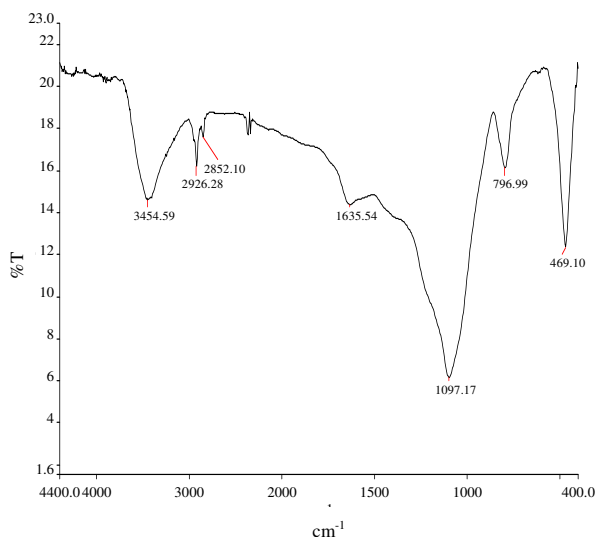


Figure 2b. IR Spectrum of AcTAP (after fluoride loaded)

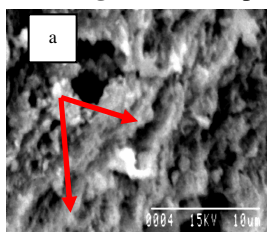


Figure 3a. Scanning electron microscopy of activated tea ash before passing fluoride solution. a) No cluster found.

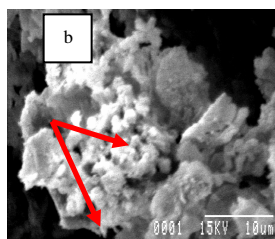


Figure 3b. Scanning electron microscopy of activated tea ash after passing fluoride solution. b) Cluster found.

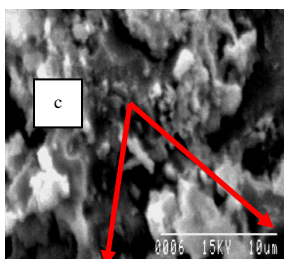


Figure 3c. Scanning electron microscopy of activated tea ash after regeneration of. c) After regeneration no cluster found

Effect of pH

The effect of pH on the fluoride removal from aqueous solution by using AcTAP is shown in Figure 4. This result shows that removal of fluoride ion is most appreciable in the pH range 2.0-7.0 with a peak value at pH 6.0. This may be explained by considering pH_{ZPC} (Table 1) for the AcTAP because removal of fluoride by adsorption process is highly dependent on solution pH as it can alter the surface charge of the adsorbent²⁷. Hence, in the

present work, the highest removal capacity was performed at pH 6.0, since $\text{pH}_{\text{ZPC}} = 6.5$, the surface will be positively charged. Decrease in removal capacity was observed below and above pH 6.0 (Table 2), which may be attributed to unfavorable surface charges and competition for adsorption sites due to excess anions at alkaline conditions²⁷.

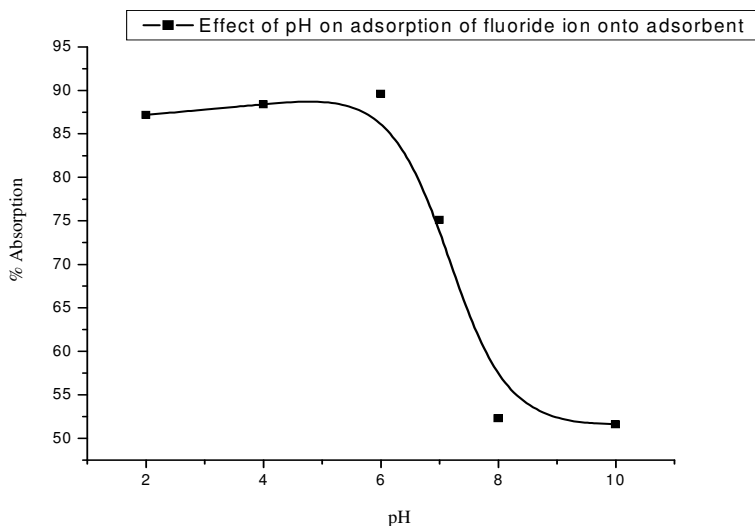


Figure 4. Effect of pH on removal of fluoride onto AcTAP (experimental conditions: Initial fluoride concentration: 5.0 mgL^{-1} , adsorbent dose: 0.8 g/L with particle size $100 \mu\text{m}$, agitation speed: 300 rpm , Contact time: 60 minutes , Temperature: 303 K)

Table 1. The main physicochemical characteristics of adsorbent

Parameter	Value Tea-waste	Activated tea waste
i. surface area, $\text{m}^2 \text{ g}^{-1}$	477.69	494.31
ii. Particle size, μm	50-300	50-300
iii. Elemental analysis, %		
C	58.33	85.6
H	7.73	5.23
N	0.44	0.35
O	32.42	12.6
S	0.51	0.14
iv. Ash content, %	4.76	5.33
v. Moisture content, %	5.66	2.11
pH_{ZPC}		6.5

Table 2. Effect of pH on adsorption of fluoride by AcTAP

pH of the solution	$q_e, \text{mg g}^{-1}$
2.0	5.45
4.0	5.52
6.0	5.59
7.0	4.69
8.0	3.27
10.0	3.22

Effect of particle size and adsorbent dose

Particle size is an important factor in adsorption because adsorption is a surface phenomenon and the extent of adsorption is expected to be proportional to the surface area available for adsorption²⁶. In the present work, the effect of adsorbent particle size was investigated by using the average particle size (50,100,150,200,250 and300 μm) (Figure 5). Increase in particle size from 50 to 300 μm reduces the adsorption level from 89.6 to 77.8 percent. It may be due to the smaller particle size of adsorbent gives large surface area, increases the adsorption capacity¹. The effect of adsorbent dose on fluoride adsorption was studied at fixed initial concentration (5 mg L^{-1}) (Figure 6). The extent of percentage of adsorption increased with increase in the adsorbent dose while loading capacity (amount of fluoride adsorbed per g of the adsorbent) gradually decreased for decreasing the number of interaction site between the adsorbent and adsorbate. This is probably due to increase of adsorption sites²⁸⁻²⁹. From the trend it appears that a maximum level (51.3 to 97.6 %) of fluoride adsorption occurs with increase in adsorbent dose from 0.2 to 2.4 g L^{-1} and then the adsorption is not changed with the adsorbent dose due to establishment of equilibrium condition²⁷. Distribution coefficient (K_{DC}) usually calculated in this study to define the partitioning of an element in a system. Distribution coefficient reflects the binding capacity of the surface for adsorption. It is expressed by using the following equation³⁰.

$$K_{\text{DC}} = \frac{\text{anion}_{\text{ads}}}{\text{anion}_{\text{diss}}} \frac{1}{C_p} \quad (3)$$

In the present study the value of K_{DC} increased with increase of adsorbent dose at a constant pH (Figure 7) which indicates the heterogeneous nature of the adsorbent surface.

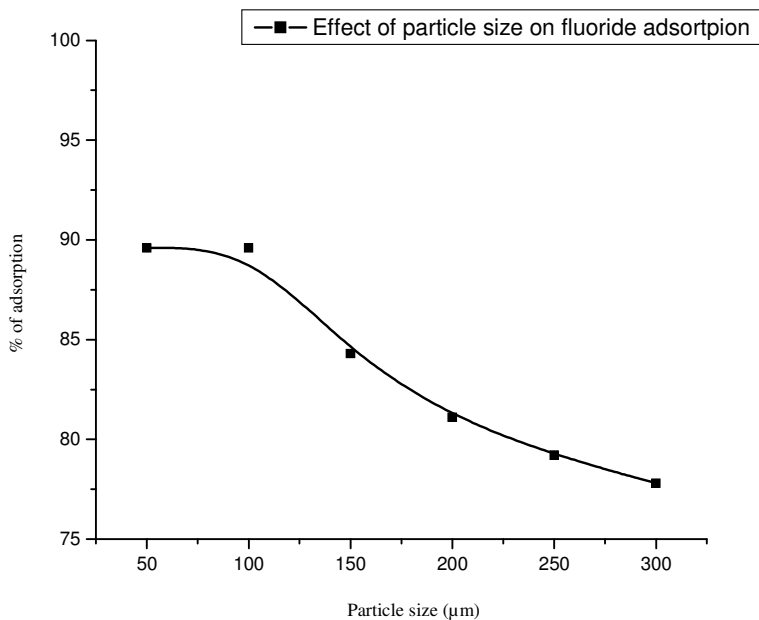


Figure 5. Effect of particle size on the adsorption of fluoride by AcTAP (experimental conditions: Initial fluoride concentration: 5.0 mgL^{-1} , pH: 6.0, adsorbent dose: 0.8 g/L , agitation speed: 300 rpm, Contact time: 60 minutes, Temperature: 303 K)

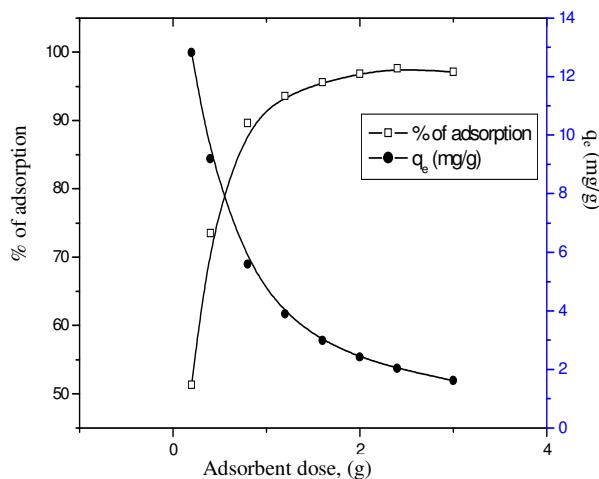


Figure 6. Effect of Adsorbent dose on the adsorption of fluoride by AcTAP (experimental conditions: Initial fluoride concentration: 5.0 mgL^{-1} , pH: 6.0, particle size: $50 \mu\text{m}$, agitation speed: 300 rpm, Contact time: 60 minutes, Temperature: 303 K)

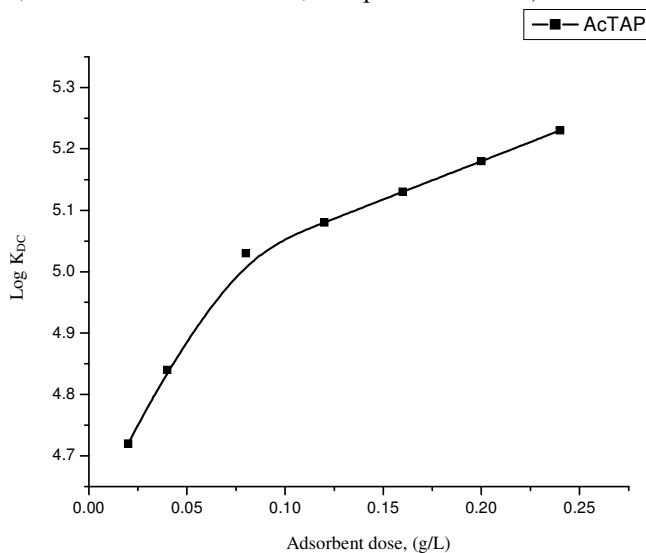


Figure 7. Plot of distribution coefficient vs. adsorbent dose (experimental conditions: Initial fluoride concentration: 5.0 mgL^{-1} , pH: 6.0, particle size: $50 \mu\text{m}$, agitations speed: 300 rpm, Contact time: 60 minutes, Temperature: 303 K)

Effect of agitation speed

Studies on the effect of agitation speed were conducted by varying speeds from 100 to 400 rpm, at optimum pH of 6.0 with adsorbent dose of 2.4 g L^{-1} and contact time of 60 min at 303 K (Figure 8). At a given time, fluoride removal increases with the increase in the speed of agitation. The reason for the increase is the diffusion of adsorbate towards the adsorbent surface³¹ and also better contact between the adsorbent and adsorbate is possible³². Similar findings for fluoride removal by using activated charcoal have been reported by other investigator³².

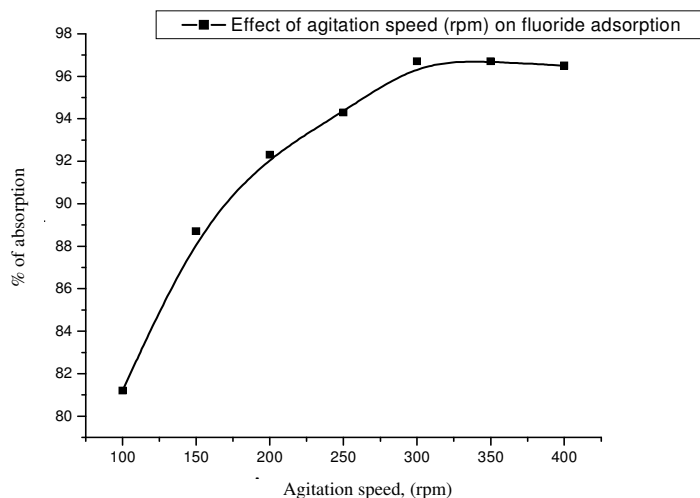


Figure 8. Effect of agitation speed on removal of fluoride onto AcTAP (experimental conditions: Initial fluoride concentration: 5.0 mg L^{-1} , pH: 6.0, adsorbent dose: 2.4 g/L and particle size $50 \mu\text{m}$, agitation speed: 300 rpm, Contact time: 60 minutes, Temperature: 303 K)

Effect of contact time and adsorption kinetic model

The adsorption rate of fluoride at different initial concentrations (5.0 , 10.0 and 50.0 mg L^{-1}) was investigated by varying the time ranging from 40 to 300 min (Figure 9). Figure 10 also shows that with a fixed amount of AcTAP, the adsorption of fluoride increased with time and then attained equilibrium after 180 min at different initial concentrations indicating the independent nature of time to reach equilibrium conditions. Figure 9 also indicate initial adsorption is very rapid and slow approach to equilibrium. A similar finding has been reported for removal of fluoride onto lanthanum incorporated chitosan beads^{27,29}.

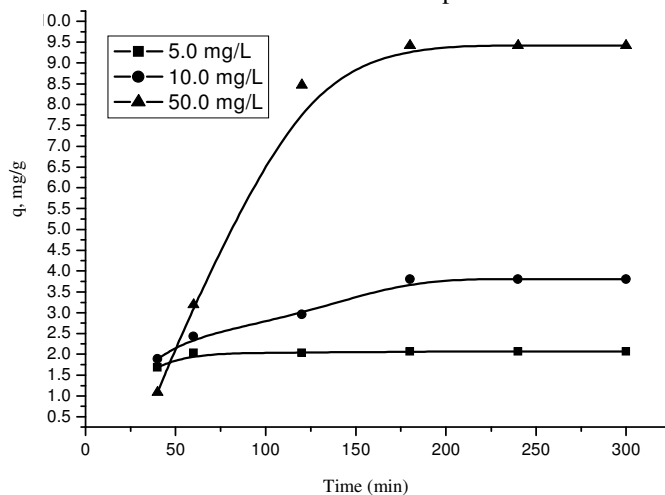


Figure 9. Effect of contact time on removal of fluoride onto AcTAP at various concentrations (experimental conditions: pH: 6.0, adsorbent dose: 2.4 g/L and particle size $50 \mu\text{m}$, agitation speed: 300 rpm, Temperature: 303 K)

In the present study, two main types of kinetic models *viz.* reaction-based models and diffusion based models²⁷ were frequently used to determine various kinetic parameters of the adsorption system. The experimental data was analyzed by application of the sorption kinetics pseudo-first-order and pseudo-second-order kinetic models. A simple pseudo-first order kinetic model also known as Lagergren equation is presented as²⁷.

$$\log(q_e - q_t) = \log q_e - \frac{k_1 t}{2.303} \quad (4)$$

Where, q_e is equilibrium F⁻ concentration on adsorbent (mg g^{-1}) and q_t is amount of F⁻ adsorbed at time t (mg g^{-1}), k_1 is pseudo-first-order rate constant (min^{-1}). The rate constants were calculated from the linearized plots of $\log(q_e - q_t)$ vs. t . The pseudo-second-order model is commonly used as²⁷

$$\frac{t}{q_t} = \frac{1}{k_2 q_e^2} + \frac{t}{q_e} \quad (5)$$

$$h = k_2 q_e^2 \quad (6)$$

Where, k_2 is pseudo-second-order rate constant ($\text{g mg}^{-1} \text{min}^{-1}$) and h = initial adsorption rate ($\text{mg g}^{-1} \text{min}^{-1}$). The values of kinetic parameters and correlation coefficients of the adsorption kinetic models obtained from the linear plots of t/q_t vs. t are presented in Table 3. It is apparent from the values of correlation coefficients that the fitness of the pseudo-second-order model is better as compared to pseudo-first-order model. Additionally, comparing the experimental removal capacities ($q_{e,\text{exp}}$) and calculated values ($q_{e,\text{cal}}$) at different initial concentrations the experimental results obey the pseudo second-order model. The adsorption capacities at different initial concentrations varying with contact time are shown in Figure 10. By pore diffusion or particle diffusion model, sorption of a liquid adsorbate on porous solid adsorbent can be determined. This model can be written as:

$$B = \frac{\pi^2 D}{r^2} \quad (7)$$

Where B (pore diffusion coefficient) is determined as the slope of the plots of B_t vs. t (Figure not shown) at different initial fluoride concentrations by using equation:

$$B_t = -0.4997 - \ln \left(1 - \frac{q_t}{q_e}\right) \quad (8)$$

According to³³, intraparticle diffusion model is commonly used to characterize the sorption data and be expressed as:

$$q_t = K_1 t^{0.5} + I \quad (9)$$

Table 3. Kinetics parameters for adsorption of fluoride by AcTAP at different initial concentrations

Different initial conc., mg L^{-1}	$q_{e,\text{exp}}$, mg g^{-1}	Pseudo-first-order kinetic model			Pseudo-second-order kinetic model			
		$q_{e,\text{cal}}$, mg g^{-1}	k_1 , min^{-1}	R^2	$q_{e,\text{cal}}$, mg g^{-1}	k_2	h , $\text{mg g}^{-1} \text{min}^{-1}$	R^2
5.0	2.07	0.23	0.002	0.005	2.11	0.08	0.36	0.99
10.0	3.81	3.66	0.008	0.238	4.58	0.04	0.08	0.99
50.0	9.42	3.87	0.002	0.088	14.95	0.005	0.1	0.82

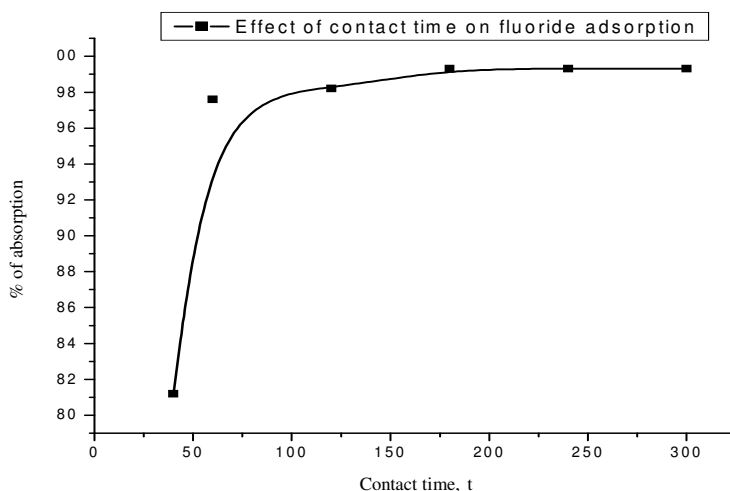


Figure 10. Effect of contact time on removal of fluoride onto AcTAP (experimental conditions: Initial fluoride concentration: 5.0 mgL^{-1} , pH: 6.0, adsorbent dose: 2.4 g/L and particle size $50 \mu\text{m}$, agitation speed: 300 rpm, Temperature: 303 K)

Where, K_i is intraparticle diffusion coefficient and I intraparticle diffusion is model constant. Table 4 shows that the diffusion coefficient values decreased with increasing initial fluoride concentrations due to decreasing of available open sites to adsorption³⁴ whereas intraparticle diffusion rate increased with this order. The values of correlation coefficients (R^2) for particle diffusion model are closer to unity supporting that particle diffusion of fluoride adsorption is contributing more towards rate controlling step. However, in case of intraparticle diffusion model, plots did not pass through the origin (the intercept values are between 0.024 and 0.775) which indicates that the adsorption of fluoride on AcTAP is a complex process involving surface adsorption. Simultaneously, the increase in intercept values of intraparticle diffusion model with increasing initial concentrations indicates increasing of boundary layer effect.

Table 4. Pore diffusion and intraparticle rate parameters at different initial fluoride concentrations

Concentration, mg L^{-1}	Pore diffusion coefficient	R^2	Intraparticle diffusion coefficient	R^2
5.0	2.77×10^{-4}	0.95	0.024	0.94
10.0	2.28×10^{-6}	0.96	0.186	0.91
50.0	1.77×10^{-8}	0.98	0.775	0.82

Effect of initial concentration

The adsorption of fluoride onto AcTAP was conducted by varying initial fluoride concentration using optimum adsorbent dose (2.4 g L^{-1}) with $50 \mu\text{m}$ particle size, pH 6.0, agitation speed 300 rpm at temperature 30°C for a contact time of 180 min. The percentage removal of fluoride decreased with increase in initial fluoride concentration (Figure 11) and showed a little decrease at higher concentrations having a limited number of active sites. This is probably due to increase the ratio of ions/adsorbent and also saturated the higher energy sites, adsorption begins on lower energy sites, resulting decreases in the adsorption efficiency³⁵ Figure 11 also shows the amount of adsorbed fluoride increased with increase in initial concentrations due to increasing concentration gradient acts as increasing driving force to overcome all mass transfer resistances of the fluoride between the aqueous and solid phase, leading to an increasing equilibrium sorption until sorbent saturation is achieved¹.

Effect of temperature

It is well established that temperature is an additional factor greatly influence any adsorption process. The effect of solution temperature was investigated at 303, 313, 323 and 333 K. The results summarized in Figure 12, indicating the adsorption rate decreased with increase in temperature. This result indicates low temperature favours the removal of fluoride molecules by adsorption onto AcTAP as well as the adsorption process is exothermic in nature. The decreasing of removal may be due to at high temperature the thickness of the boundary layer decreases due to increased tendency of the molecules to escape from the adsorbent surface to the solution phase, which results in a decrease in the adsorption capacity as temperature is increased³⁶. Similar results were previously reported by³⁷.

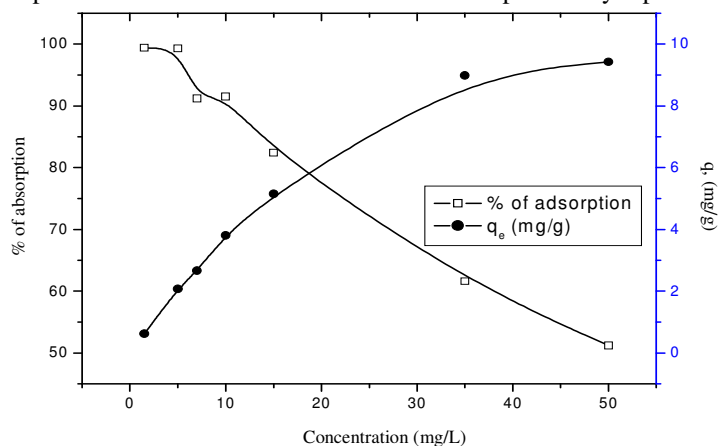


Figure 11. Effect of initial concentrations on the removal of fluoride onto AcTAP (experimental conditions: pH: 6.0, adsorbent dose: 2.4g/L and particle size 50 μm , agitation speed: 300 rpm, contact time: 180 minutes, Temperature: 303K)

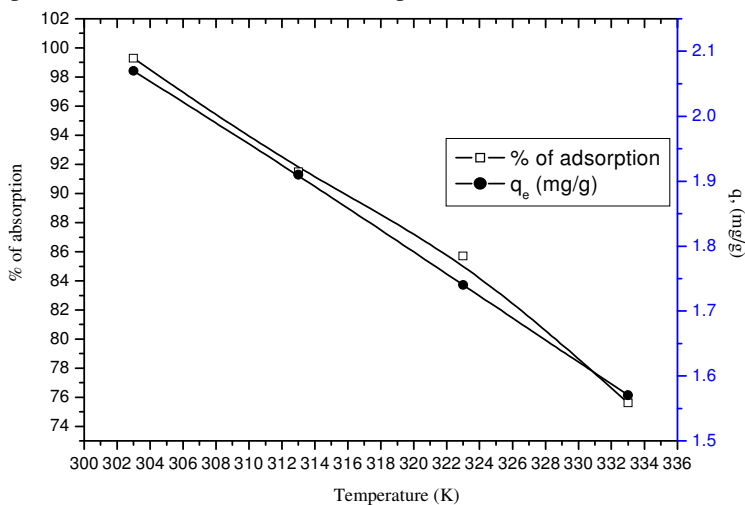


Figure 12. Effect of temperature on the removal of fluoride onto AcTAP (experimental conditions: Initial fluoride concentration: 5.0 mgL^{-1} , pH: 6.0, adsorbent dose: 2.4 g/L and particle size 50 μm , agitation speed: 300 rpm, contact time 180 min, Temperature: 303 K)

Adsorption isotherms

Analysis of data by adsorption isotherms is very important to design of a adsorbent and for calculating the adsorption efficiency of the adsorbent systems. In this study Langmuir, Freundlich, D-R and Tempkin adsorption isotherm models are analyzed and mathematical expressions of these models are given in Table 5.

Table 5. Mathematical equations of different isotherm models

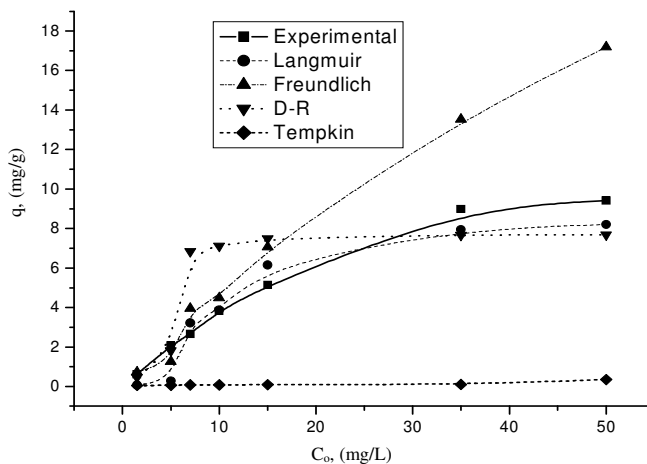
Isotherm models	Mathematical equations	Plots	Ref
Langmuir	$\frac{1}{q_e q} = \frac{1}{q_{\max} K_L C_e} + \frac{1}{q_{\max}}$ (9)	1/q _e vs. 1/C _e	[43]
Freundlich	$\log q_{eq} = \log K_F + \frac{1}{n} \log C_e$ (10)	log q _e vs. log C _e	[27]
Dubinin-Radushkevich (D-R)	$\ln q_e = \ln q_m - \beta \varepsilon^2$ (11)	ln q _e vs. ε ²	[43]
Tempkin	$q_e = B \ln A + B \ln C_e$ (12)	q _e vs. ln C _e	[26]

The linear equation of Langmuir model plotted 1/q_e vs 1/C_e gives a straight line (R² = 0.995 to 0.983) at different temperatures, indicating that Langmuir adsorption is followed by the adsorption very well data at all temperatures. The values of Langmuir constant (K_L) and maximum adsorption capacity (q_m) were calculated from the slope and intercept of the plots at different temperatures are reported in Table 6. With increasing temperature, the values of both K_L and q_m (adsorption capacity) are decreased indicating higher temperature induces lower adsorption capacity³⁸. The Freundlich adsorption isotherm is based on heterogeneity of the surface³⁹ for the fluoride removal by adsorption. Freundlich constant is K_f and n is another constant informing the degree of heterogeneity of the surface sites⁴⁰. The values of K_f and 1/n have been evaluated from the graph by plotting log q_e vs. log C_e and compiled in Table 6. The values of n between 1 and 10 represents a favorable adsorption and for the present study according to this model the value of n also presented the same trend of beneficial adsorption. The high correlation coefficients (R²) and maximum adsorption capacity values at all temperatures indicate the adsorption data of fluoride ions onto AcTAP better fitted with the Langmuir equation and suggests the monolayer uniform adsorption. Figure 13 also supports this but in case of lower fluoride concentration adsorption process followed by both Langmuir and Freundlich isotherm models. The essential characteristics of this model can be expressed in terms of a dimensionless parameter, separation factor (R_L) which describes the type of adsorption⁴¹ and is calculated by $R_L = \frac{1}{1 + K_L C_i}$. The values of R_L were 0.17 to 0.28 at different temperatures representing highly favourable adsorption of fluoride ions onto AcTAP. The D-R isotherm is widely used to determine the physical or chemical adsorption phenomenon and related to heterogeneity of energies over the surface⁴¹. The estimated value of E_s from the constants (β) of D-R isotherm model using equation ($E_s = \frac{1}{\sqrt{2\beta}}$, where β = D-R constant) ranging from 5.01 to 1.42 at different temperatures for present study were found in the range expected for physical adsorption³⁸. Table 6 also shows that the constant (A), maximum adsorption capacity (q_m) and correlation coefficient values lower at higher temperature. By plotting q_e vs. ln C_e, the Tempkin constants were calculated from the linear equation and these values with correlation coefficients at different temperatures are also reported in Table 6.

Table 6. Adsorption isotherm constants for adsorption of fluoride by AcTAP at different temperatures

Tem p(K)	Langmuir isotherm				Freundlich			D-R			Tmkin			
	K_L	R_L	q_m	R^2	K_f	n	R^2	q_m	B	E_s	R^2	B	A	R^2
303	0.97	0.17	8.55	0.999	4.83	2.5	0.93	7.67	0.019	5.01	0.92	1.85	0.08	0.89
313	0.61	0.24	7.81	0.993	2.83	1.96	0.92	7.08	0.043	3.40	0.85	2.49	0.01	0.83
323	0.55	0.27	7.15	0.948	1.24	1.24	0.919	7.11	0.14	1.91	0.82	3.51	0.002	0.82
333	0.28	0.41	7.03	0.912	0.72	1.19	0.908	5.48	0.25	1.42	0.71	3.78	0.001	0.81

Tempkin constant (A, Tempkin constant related to equilibrium binding constant ($L\ mg^{-1}$) and B is Tempkin constant related to the heat of adsorption) determines the heat of adsorption. In comparing the experimental results with different isotherm models are plotted in Figure 13 which also indicates the better fitness of adsorption data to the Langmuir adsorption isotherm. This result suggests that the adsorbed fluoride ions did not compete each other and ions were adsorbed by forming a monolayer onto AcTAP. Table 7 summarizes the comparison of the maximum fluoride adsorption capacities of various sorbents including present study and shows that AcTAP has high adsorption capacity of fluoride than other reported adsorbents, reflecting a promising utility for AcTAP utilization in fluoride removal from contaminated water.

**Figure 13.** Comparison between the measured and modeled isotherm profiles for the removal of fluoride by using AcTAP on different initial concentration (mgL^{-1}): (experimental condition pH of the solution: 6.0, adsorbent dose: 2.4g/L, particle size: 50 mm, agitation speed: 300 rpm, contact time: 180 minutes, temperature: 303 K)**Table 7.** Previously reported adsorption capacity of various types of waste biomass for fluoride

Name of adsorbent	Adsorption capacity, $mg\ g^{-1}$	Reference
Cynodon dactylon	4.75	[44]
Tamarind seed	6.09	[1]
Used Tea powder	0.05	[45]
Activated carbon from <i>Acacia Arabica</i>	2.06	[46]
AcTAP	8.55	Present study

Adsorption kinetics

In order to investigate the kinetic of process such as the mechanism of adsorption and potential rate controlling steps, basically the order of process has to be studied. From the Table 3, it is clear that the fluoride adsorption process is entirely followed pseudo-second order kinetics. Many publication were also studied the kinetic order of adsorption process onto solid support which could use as primary data to propose the possible adsorption mechanism, leading to understanding of adsorption nature of fluoride onto solid support⁴².

Activation energy and thermodynamic study

The activation energy (E_a) for fluoride ions adsorption onto AcTAP was calculated by using Arrhenius equation:

$$\ln k = \ln A - \frac{E_a}{RT} \quad (13)$$

E_a value ($E_a = 32.01 \text{ kJ mol}^{-1}$) calculated from the slope of a plot of $\ln k$ vs. $1/T$ (Figure 14). The magnitude of activation energy gives an idea about the type of adsorption. According to literature³⁸, this E_a value indicates that the fluoride ions adsorption process is physical adsorption in nature. This result corresponds well with those from D-R isotherm. Thermodynamic parameters associated with the adsorption process *viz.* Gibb's free energy change (ΔG^0), enthalpy change (ΔH^0) and entropy change (ΔS^0) were calculated using the following equations:

$$K_c = \frac{C_{Ac}}{C_e} \quad (14)$$

$$\Delta G^0 = RT \ln K_c \quad (15)$$

$$\log K_c = \frac{\Delta S^0}{2.303R} - \frac{\Delta H^0}{2.303RT} \quad (16)$$

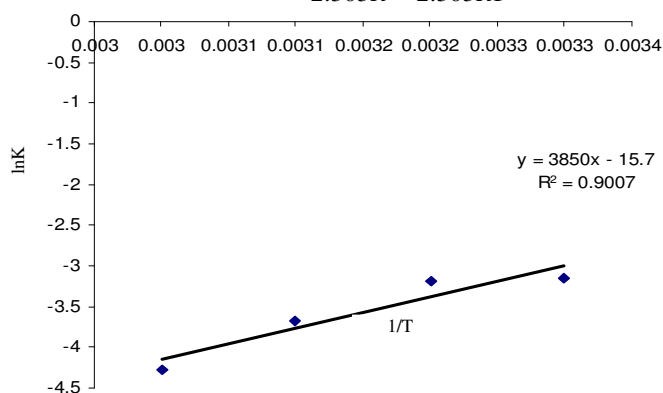


Figure 14. Arrhenius equation plot for removal of fluoride onto AcTAP

The values of ΔH^0 and ΔS^0 obtained from the slope and intercept by plotting $\log K_c$ vs. $1/T$ (Figure 15) are shown in Table 8. The negative value of ΔG^0 at all temperatures indicates the feasibility of the fluoride ions adsorption and the process is spontaneous in nature. Lower values of ΔG^0 with increasing temperature supports adsorption easier at lower temperature. The negative value of ΔH^0 suggests the exothermic nature of adsorption process and the negative value ΔS^0 shows the process is enthalpy driven.

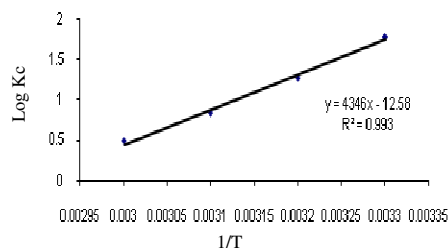


Figure 15. Thermodynamic plot $\log K_0$ vs. $1/T$ for removal of fluoride onto AcTAP

Table 8. Activation energy and thermodynamic parameters for adsorption of fluoride by AcTAP

E_a kJ mol ⁻¹	ΔG^0 , kJ mol ⁻¹				ΔH^0 , kJ mol ⁻¹	ΔS^0 kJ mol ⁻¹
32.01	303 K	313 K	323 K	333 K	-83.21	-0.241
	-10.19	-7.78	-5.37	-2.96		

Desorption study

Desorption study helps to elucidate the adsorption and recycling of the spent adsorbent and the adsorbate. Different regeneration media like 25% NaOH and 1(N) HCl were used for desorption of fluoride. The desorption of adsorbed fluoride on AcTAP resulted about 91.68%.

Field data analysis

With a view to making use of the adsorbent in practical applicability of AcTAP for defluoridation in actual field conditions, the AcTAP was tested with fluoride contaminated groundwater collected from affected area of Birbhum district in West Bengal, India. The physicochemical characteristics of groundwater sample are shown in Table 9. The results show that the F^- levels in the ground water samples collected from study area decreased to $<1 \text{ mg L}^{-1}$, which is well below the limits of WHO drinking water standards³. Comparing the fluoride removal by AcTAP from synthetic solution and field groundwater indicates that there is no significant difference suggesting AcTAP can be exploited for defluoridation in both household and community level and thus the use of AcTAP is a thoughtful and economic attempt for its valuable, necessitous and needy utilization for contaminated groundwater treatment process in affected areas.

Table 9. Physicochemical analysis of groundwater samples collected from study area (Nowpara)

Parameters	Nowapara
pH	7.7
Conductivity, mS cm ⁻¹	3.0
Fluoride, mg L ⁻¹ as (F ⁻)	10.0
Total hardness, mg L ⁻¹ as Ca and Mg	40.0
Chloride, mg L ⁻¹ as (Cl ⁻)	31.48
Sulphate, mg L ⁻¹ as (SO ₄ ⁻²)	112.2
Phosphate, mg L ⁻¹ as (PO ₄ ⁻²)	0.048
Ammonical nitrogen, mg L ⁻¹	0.095
COD, mg L ⁻¹	24.0
Iron, mg L ⁻¹ as Fe ⁺²	0.153

Conclusion

A new medium, waste tea ash has been developed for fluoride removal in this study. Numerous advantages of the waste tea ash make the waste an excellent adsorbent for removal of fluoride from aqueous solution under acidic pH and further increases of pH showed less adsorption. The adsorption process nicely fitted with Langmuir adsorption isotherm indicating monolayer adsorption and adsorption of fluoride decreased with increase in temperature in the range of 303-333 K. Again the adsorption process was observed to follow a pseudo-second-order kinetic model and correlation coefficient values for particle diffusion model are closer to unity suggests that particle diffusion of fluoride adsorption is more towards the rate controlling step than intraparticle diffusion model. Moreover, distribution coefficient results indicate the heterogeneous nature of adsorption surface. Thermodynamic data indicates that reaction favors at lower temperature, exothermic in nature and enthalpy driven. It was also shown that tea ash has enough potential to remove fluoride (8.55 mg g^{-1}) from aqueous solution and subsequently 91.68 % fluoride can be regenerated from the adsorbent surface. Therefore, the activated tea ash is promising material for fluoride removal from aqueous solution as well as contaminated groundwater.

Acknowledgement

The authors are grateful to Dr. Alope Ghosh, Reader, Department of Chemistry, Burdwan University, Burdwan, West Bengal, India for recording FTIR data and they also extend their gratitude to Dr Srikanta Chakraborty, In charge of SEM, USIC, University of Burdwan, West Bengal, India for SEM study.

References

1. Murugan M and Subremanian E, *J Water Health*, 2006, **4**, 453-461.
2. Karthikeyan M and Elango K P, *Indian J Chem Technol.*, 2008, **15**, 525-532.
3. WHO, 2006, World Health Organization, Geneva.
4. Miretzky P, Munoz C and Carrillo-Chavez A, *J Environ Chem.*, 2008, **5**, 68-72.
5. Venkata Mohan S, Ramanaiah S V, Rajkumar B and Sarma P N, *J Hazard Mater.*, 2007, **141**, 465-474.
6. Chauhan V S, Dwivedi P K and Iyengar L, *J Hazard Mater.*, 2007, **139**(1), 103-107.
7. Das N, Pattanaik P and Das R, *J Colloid Interface Sci.*, 2005, 292, 1-10.
8. Teng S X, Wang S G, Gong W-X, Liu X-W and Gao B-Y, *J Hazard Mater.*, 2009, **168**, 1004-1011.
9. Li Y H, Wang S, Zhang X, Wei J, Xu C, Luan Z and Wu D, *Mater Res Bull.*, 2003, **38**, 469-476.
10. Maruthamuthu M and Venkatanarayana R, *Fluoride.*, 1987, **20**, 109-112.
11. Shirke P A. and Chandra P, *Fluoride.*, 1991, **24**, 109-112.
12. Sinha J, Bae J T, Park J P, Kim K H, Song C H and Yun J W, *Appl Microbiol Biotechnol.*, 2001, **56**, 89-92.
13. Mohammad A, Rao R A K, Anwar S, Ahmad J and Ahmad R, *Bioresour Technol.*, 2003, **86**(2), 147-149.
14. Mondal N K, Bhaumik R, Banerjee A, Datta J K and Baur T, *Int J Environ Sci.*, 2012, **2**(3), 1643-1661.
15. Bhaumik R, Mondal N K, Das B, Roy P, Pal K C and Das C, *C.E-J Chem.*, 2011, **97**, 21-25.

16. Wafwoyo W, Seo C W and Marshall W E, *J Chem Technol Biotechnol.*, 1999, **74**, 1117-1121.
17. Vaughan T, Seo C W and Marshall W E, *Bioresour Technol.*, 2001, **78**, 133-139.
18. Sciban M, Klasnja M and Skrbic B, *J Hazard Mater.*, 2006, **136(2)**, 266-271.
19. Shukla S R, Pai R Sand Shendarkar A D, *Seperation Purif Technol.*, 2006, **47(3)**, 141-147.
20. Palma G, J Freer J and Baeza J, *Water Res.*, 2003, **37**, 4974-4980.
21. Ahluwalia S S and Goyal D, *Eng Life Sci.*, 2005, **5(2)**, 158-162.
22. Boonamnuyvitaya V, Chaiya C, Tanthapanichakoon W and Jarudilokkul S, *Sep Purf Technol.*, 2004, **35**, 11-22.
23. Farajzadeh M A and Monji A B, *Seperation Purif Technol.*, 2004, **38**, 197-207.
24. Montanher S F, Oliveria E A and Rollemberg M.C, *J Hazard Mater.*, 2005, **117**, 207-211.
25. Strik W A and van Staden J, *Botan Marin*, 2000, **43(5)**, 467-473.
26. Mondal M K, *Korean J Chem Eng.*, 2010, **27(1)**, 144-151.
27. Bansiwala A, Thakre D, Labhshetwar N, Meshram S and Rayalu S, *Colloids Surf B.*, 2009, **74(1)**, 216-224.
28. El-Said SM, *Int J Chem Technol.*, 2010, **2(2)**, 88-93.
29. Dekhil A B, Hannachi Y, Ghorbel A and Boubaker T, *J Environ Sci Tech.*, 2011, **4**, 520-533.
30. Sujana M G, Padhan H K and Anand S, *J Hazard Mater.*, 2009, **161**, 120-125.
31. Kabbashi N A, Abdurahman N H, Muyibi S A and Qudsieh I Y, *Inter J Chem Tech.*, 2009, **1(2)**, 44-51 11
32. Tembhurkar A R and Dongre S, *J Environ Sci Engg.*, 2006, **48(3)**, 151-156.
33. Weber W J and Morris J C, *J Sanit Eng Div ASCE.*, 1963, **89**, 31-60.
34. Ofomaja A E, *Biores Technol.*, 2010, **101(15)**, 5868-5876.
35. Zouboulis A I, Lazaridis N K and Matis K A, *J Chem Tech Biotechnol.*, 2002, **77**, 958-964.
36. Bhatti H N, Nasir A W and Hanif M A, *Desalination*, 2010, **253(1-3)**, 78-87.
37. Sujana M G and Anand S, *Desalination*, 2010, **267**, 222-227.
38. Chowdhury S, Misha R, Saha P and Kushwaha P, *Desalination*, **2011, 265(1-3)**, 159-168.
39. Ruthven D M, Wiley-Interscience, New York, 1984, 433.
40. Rao M V B, Rao M S, Prasanthi V and Ravi M, *Rasayan J Chem.*, 2009, **2**, 525-530.
41. Solangi I B, Memon S and Bhangar M I, *J Hazard Mater.*, 2009, **171(1-3)**, 815-819.
42. Wanchanthuek R and Thapol A, *J Environ Sci Tech.*, 2011, **4**, 552-559.
43. Islam M and Patel R K, *J Hazard Mater.*, 2007, **143**, 303-310.
44. Alagumuthu G, Veeraputhiran V and Venkataraman R, *Archiv Appl Sci Res.*, 2010, **2(4)**, 170-185.
45. Munavalli G R and Patki V K, *J Inst Pub Health Engs.*, 2009, **10**, 36-43.
46. Ramu A, Kannan N and Srivathsan S A, *Ind J Environ Health*, 1992, **34(3)**, 192-199.